Mansoura Engineering Journal

Volume 48 | Issue 3 Article 7

August 2023

Part 2: proposed buckling factor for columns in braced and unbraced frames with composite girders

S.A. Eltawil
Structural Engineering department, Faculty of Engineering, Mansoura University, Egypt,
saraeltawil1@yahoo.com

N.S. Mahmoud
Structural Engineering department, Faculty of Engineering, Mansoura University, Egypt

S.M. Abdrabou
Structural Engineering department, Faculty of Engineering, Mansoura University, Egypt

ORIGINAL STUDY

Part 2: Proposed Buckling Factor for Columns in Braced and Unbraced Frames with Composite Girders

Sara A. Eltawil*, Nabil S. Mahmoud, Saad M. Abdrabou

Structural Engineering Department, Faculty of Engineering, Mansoura University, Egypt

Abstract

In both braced and unbraced frames, the influence of composite girders on modified buckling factor values was investigated, and the composite girders' far end were represented as hinges. Furthermore, based on the proposed stiffness parameter, the derived formulation follows the same assumptions as the standard effective length factor (K-factor). Moreover, the suggested buckling factor equations for composite girders in braced and unbraced frames were obtained using the slope-deflection method. Concerning the unbraced frame, the proposed buckling factor of columns restrained by the composite girder improves the effective length calculation and makes for a more accurate and cost-effective design than the buckling factor of columns restrained by the steel girder. Eventually, there is a slight improvement in the proposed buckling factor of columns in braced frames with the composite girder than the buckling factor of columns restrained by the steel girder, but still more accuracy than the conventional solution.

Keywords: Stability functions, Side sway permitted, Sagging moment, The alignment charts, Side sway prevented, Composite girders, Stiffness coefficients, 15% cracked analysis, Composite frames

1. Introduction

Steel-concrete composite structures are made of two different materials that are treated as a single element. This combination has a number of benefits such as resulting in steel-concrete composite structures having a high market sales in many countries (Korkess et al., 2009; Mbc, 2014) and being widely used in continuous-frame construction, especially continuous composite beams. Furthermore, The main advantages of utilizing steel-concrete composite structures are: The efficient use of structural materials, quick construction, lower dead weight, great fire performance and high rigidity (Kostic et al., 2011; Vasdravellis et al., 2012; Chang et al., 2017). Due to the additional benefits associated with just a redistribution of internal forces across the component and the simplicity with which serviceability criteria may be achieved, continuous composite beams are frequently used in buildings and bridges as an affordable structural solution. However, because continuous composite beams behave differently in the positive (also known as sagging) and negative (also known as hogging) moment zones, designing and analyzing them can be complex (Vasdravellis et al., 2012; Nie et al., 2004). Furthermore, creep and shrinkage of concrete will vary the force distribution through the span in hyperstatic structures such as continuous composite beams and composite frames, possibly exacerbating concrete cracking in negative bending zones (Fan et al., 2010).

Negative bending moments in continuous composite beam interior support sections generate tension in the concrete slab and compression in the steel, which is unsavory in the design. A number of studies have been conducted to produce models for analyzing the behavior of composite beams, the bulk of which focused on beams with positive bending moments. A few studies examined the crack propagation in concrete slabs and the ultimate bearing capacity of composite beams during hogging moments (Kostic et al., 2011; Chen et al., 2014).

Received 24 October 2022; revised 5 March 2023; accepted 22 March 2023.
Available online 28 August 2023

* Corresponding author.
E-mail addresses: saraeltawil1@yahoo.com (S.A. Eltawil), Abdrabou@mans.edu.eg (N.S. Mahmoud), nsm_eco@yahoo.com (S.M. Abdrabou).

https://doi.org/10.58491/2735-4202.3062

Studying how composite beams behave under negative moments is essential. We haven't come across many experimental investigations in this topic. The efficiency of the shear connection while the slab is under tension is not well known. Nevertheless, current experimental data on composite steel-concrete beams under negative bending are theoretically evaluated using the finite element program ANSYS (Nie et al., 2004). It is proposed a method for studying the service load of continuous composite beams. With this technique, we must perform time-dependent and short-term evaluations, accounting for the concrete slab's shrinkage, creeping, and cracking (Bradford et al., 2002).

Due to the nonlinearities in each structural element, including the steel sections, reinforced concrete slabs, and shear connectors, composite girder behavior generally demonstrates substantial nonlinearity. Additionally, because to the complexity of composite structures, nonlinear analysis and computer programs are crucial for studying them. The usage of linear-elastic analysis in Eurocode 4 (EC4), however, is proposed to accommodate for existing nonlinearities and simplify design (Kostic et al., 2011). Concrete cracking reduces flexural stiffness in hogging moment zones though not in sagging zones whenever the extreme-fiber tensile stress in concrete approaches double the mean value of the axial tensile strength recommended by EN 1992-1-1 (Tikka and Mirza, 2014). Moreover, elastic analysis must take relative stiffness variation into consideration. The length of the cracked zones in beams in braced frames is fixed (Eurocode 4 recommends that the cracked region be 0.15 of the beam length). Software analysis under design loads is the only way to determine the incidence of cracking in unbraced frames (Johnson, 2011). Actually, Eurocode 4 [27] gives a few simple methods for estimating creep, concrete cracking, and shear lag effects. Using the computer program "Kontinualac," four composite girders that are considered to be fully connected [28] were numerically assessed and the results compared. From this comparison, it is found that the zone of cracked concrete indicated by "cracked" analysis was much less than the length anticipated in 15 percent cracked analysis (Kostic et al., 2011).

One of the most important applications in the field of second order analysis and members slenderness is the calculation of the effective length factor in structural engineering (Al-Ghalibi, 2014). Additionally, the behavior of structural analysis as well as the cost of using cross sections are obviously affected by the buckling length of steel frame columns (Ali, 2012). For braced and sway frames, most codes (AISC, 2016) (AISC, 2010), Egyptian Design Code of Steel Construction and bridges ([Load and resistance factor design (LRFD), 2008] and [Allowable stress design (ASD), 2009]) (M. of Housing, 2001, M. of Housing, 2007) use alignment charts to determine the buckling length factor (K). Furthermore, by changing an end-restrained compression member to an equivalent pinned-ended member, the K-parameter is employed to simplify frame member design. Additionally, the effective length factor is estimated numerically using exact equations or by using alignment charts (Fig. 1) (Moustafa and Salama, 2015). Simpler equations and charts are utilized in most design specifications in practical applications to estimate the effective lengths of

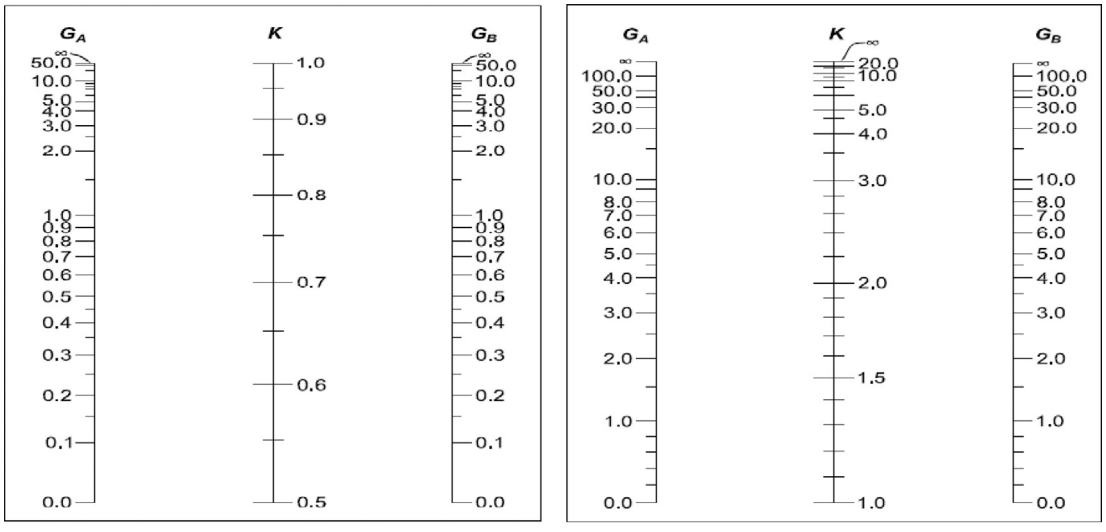

Fig. 1. Alignment charts for effective length factor.

frame columns (Fan et al., 2010). The French Design Rules for Steel Structures have featured simple equations since 1966; these rules have now been adopted by the European Recommendation for Steel Construction (Duan and Chen, 1999). In order to get more precise closed form formulae for computing the effective length factors in respect to rotational resistance at the column ends, the French rule equations are developed (Moustafa and Salama, 2015). A new buckling length factor (K) formula was also made in order to precisely calculate the stiffness of column ends (Ali, 2012).

By modifying some of the outdated assumptions of the traditional approaches, it is possible to derive approximate equations for estimating the effective length factor on the basis of the suggested procedures (Al-Ghalibi, 2014). On top of that, a mathematical method is provided for determining the K-factor for braced and unbraced frames, which consists of columns and tapered girder with varying far end conditions (King et al., 1993). In addition, the NCCI article SN008a to BS EN1993-1 includes a simple formula to calculate effective column lengths in steel frames with multiple stories (da Silva et al., 2010, Webber et al., 2015a). We provide a straightforward method for approximating buckling loads in braced frames (Girgin and Özmen, 2008). Five different boundary conditions for top and bottom columns are also utilized to get the effective length factor formulae, allowing for more precise design of columns in braced frames (Lian Duan and Chen, 1989a). It is recommended to use a modified alignment chart approach to determine an approximate coefficient for unbraced frame column design (Lian Duan and Chen, 1989b) (Webber et al., 2015b). Furthermore, 2960 braced simple frames subjected to short-term loads were simulated to determine how different methods of estimating the effective length factor (K) influenced column strength calculations (Tikka and Mirza, 2014).

In this paper, Proposed column buckling factor equations are suggested for braced and unbraced columns in frames with composite girders. Moreover, girders' far-end conditions are represented as hinged. Also, the derivation is also applied to continuous composite beams with varying flexural stiffness in braced and unbraced frames since the phenomenon of concrete cracking reduces flexural stiffness in hogging moment zones but not in sagging areas. Additionally, this derivation has taken into consideration this phenomenon. The flexural stiffnesses, both uncracked and cracked, are EI_1 and EI_2, respectively (Fig. 2). I_1: the moment of inertia for steel girder (In most cases, reinforcement is disregarded while calculating I_1.), I_2: the moment of

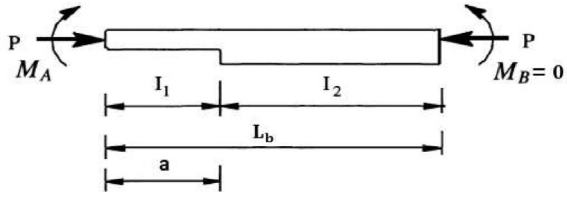

Fig. 2. Composite girder with hinged far end.

inertia for composite girder, E: Modulus of elasticity and L and a are lengths as shown in (Fig. 2).

The positions at the two ends of the beam-column are indicated by the two subscripts A and B in Table 1, whereas G is defined as:

$$G = \frac{\sum (EI/L)_{columns}}{\sum (EI/L)_{beams}}$$

where: L is the column's unsupported length.

I is the moment of inertia orthogonal to the buckling plane of the columns and beams (M. of Housing, 2001).

The suggested formulas for the k-factor:

For a composite girder, the differential equation is:

$$EIy'' = -M_a + \frac{M_a - M_b}{L} x - p\,y \tag{1}$$

where:

M_a, M_b are bending stiffness.

Coefficients of stiffness for hinged far end:

By solving the preceding equations, we are able to derive the girder stiffness coefficients: The slope-deflection equations for composite girders with hinged far ends in a braced and unbraced frame are derived. The notation (V, Y, Z, and Q) will be used to make the expressions easier to understand. In the appendix, these notations are illustrated in detail.

$$S_{NN} = \frac{-Q}{ZY - QV} \tag{2}$$

$$S_{NF} = \frac{Y}{ZY - QV} \tag{3}$$

$$S_{FN} = \frac{-Z}{QV - ZY} \tag{4}$$

$$S_{FF} = \frac{V}{QV - ZY} \tag{5}$$

Braced frame (Side sway prevented):

As shown in (4), the general formula for analyzing the stability of a braced frame made of steel columns and composite girders with a hinged far-end condition is:

Table 1. Comparison of suggested equations for the stability analysis of braced and unbraced frames with composite girders with general equations for the stability analysis of braced and unbraced frames.

Side sway mode	General equations	Suggested equations
Prevented side sway	$\frac{G_A G_B}{4}\left(\frac{\pi}{K}\right)^2+\frac{(G_A+G_B)}{2}\left(1-\frac{\pi/K}{\tan(\pi/K)}\right)+\frac{2\tan(\pi/K)}{\pi/K}=1$	$\frac{G_A G_B}{4\alpha}\left(\frac{\pi}{K}\right)^2+\frac{(\alpha G_A+G_B)}{2\alpha}\left(1-\frac{\pi/K}{\tan(\pi/K)}\right)+\frac{2\tan(\pi/K)}{\pi/K}=1$
Permitted side sway	$\frac{G_A G_B(\pi/K)^2-36}{6(G_A+G_B)}=\frac{\pi/K}{\tan(\pi/K)}$	$\frac{G_A G_B(\pi/K)^2-36\alpha}{6(\alpha G_A+G_B)}=\frac{\pi/K}{\tan(\pi/K)}$

$$\frac{G_A G_B}{4\alpha}\left(\frac{\pi}{K}\right)^2+\frac{(\alpha G_A+G_B)}{2\alpha}\left(1-\frac{\pi/K}{\tan(\pi/)}\right)+\frac{2\tan(\pi/K)}{\pi/K}=1 \quad (6)$$

$$G=\frac{\sum(EI/L)_{columns}}{\sum(EI/L)_{beams}} \quad (7)$$

Mathematical value of the stiffness modification factor:

By dividing the bending stiffness of composite girders by the bending stiffness of traditional girders, the modification factor for composite girder stiffness in braced frames is calculated.

The resulting parameter is:

When the girder's far end is hinged:

$$\alpha=\frac{1}{2V} \quad (8)$$

Unbraced frame (Side sway permitted):

As shown in (9), the general formula for analyzing the stability of an unbraced frame made of steel columns and composite girders with a hinged far-end condition is:

$$\frac{G_A G_B(\pi/K)^2-36\alpha}{6(\alpha G_A+G_B)}=\frac{\pi/K}{\tan(\pi/K)} \quad (9)$$

$$G=\frac{\sum(EI/L)_{columns}}{\sum(EI/L)_{beams}} \quad (10)$$

Mathematical value of the stiffness modification factor:

The formula for the composite girder stiffness modification factor in unbraced frames is as follows:

When the girder's far end is hinged:

$$\alpha=\frac{1}{6V} \quad (11)$$

2. Formula verification

The composite girder approaches a constant cross-sectional girder whenever the moment of inertia ratio ((I_1/I_2) is one and a and b are both zero. So that:

(1) Column modification factors in frames for a restraining composite girder are as follows:

The above equations are identical to the values provided in ECP code to account for the influence of far end conditions of restraining girders when employing alignment charts, as shown in Table 2.

(2) The proposed rotation angles at the ends of the composite girder, which are deduced for

Table 2. The modification factors of columns in frames for a restraining composite girder with hinged far end condition at constant cross-sectional girder approach.

Far end condition for composite girder	Side sway prevented	Side sway permitted
hinged far end	$\alpha = 1.5$	$\alpha = 0.5$

estimating the influence of using composite girders with hinged far end condition in braced and unbraced frames on the K-factor of columns, are equal to the rotation angles of the constant cross-section girder by using for $\Psi(u)$ and $\phi(u)$ their values from Table A-1 (Stephen and Timoshenko, 1961).

In Table 3: The two notations $\Psi(u)$ and $\phi(u)$ are defined by:

$$\Psi(u) = \frac{3}{2u}\left[\frac{1}{2u} - \frac{1}{\tan(2u)}\right] \tag{12}$$

$$\phi(u) = \frac{3}{u}\left[\frac{1}{\sin(2u)} - \frac{1}{2u}\right] \tag{13}$$

Example 1. Determine the rotation angles that are shown in Table III at 2u = 1.2 from Table A-1 (Stephen and Timoshenko, 1961) for the previous case.
Solution: From Table A-1 (Stephen and Timoshenko, 1961):
At 2u = 1.2:
$\Psi(u) = 1.1114$
$\phi(u) = 1.1979$
Reference (Stephen and Timoshenko, 1961):

$$\theta_A = \frac{M_o L}{EI}\left(\frac{\Psi(u)}{3} + \frac{\phi(u)}{6}\right)$$

$$\theta_A = \frac{M_o L}{EI}\left(\frac{1.1114}{3} + \frac{1.1979}{6}\right)$$

$$\theta_A = 0.570117\,\frac{M_o L}{EI} \tag{14}$$

$$\theta_B = \frac{M_o L}{EI}\left(\frac{\Psi(u)}{3} + \frac{\phi(u)}{6}\right)$$

$$\theta_B = \frac{M_o L}{EI}\left(\frac{1.1979}{6} + \frac{1.1114}{3}\right)$$

$$\theta_B = 0.570117\,\frac{M_o L}{EI} \tag{15}$$

$$\theta_A = \frac{M_o L}{EI}\left(\frac{1-\cos(2u)}{2u\sin(2u)}\right)$$

$$\theta_A = \frac{M_o L}{EI}\left(\frac{1-\cos\left(1.2 * \frac{180}{\pi}\right)}{1.2 * \sin\left(1.2 * \frac{180}{\pi}\right)}\right)$$

$$\theta_A = 0.570114\,\frac{M_o L}{EI} \tag{16}$$

$$\theta_B = \frac{M_o L}{EI}\left[\frac{\sin(2u)}{2u} + \left(\frac{\cos(2u)-1}{2u\tan(2u)}\right)\right]$$

$$\theta_B = \frac{M_o L}{EI}\left[\frac{\sin\left(1.2 * \frac{180}{\pi}\right)}{1.2} + \left(\frac{\cos\left(1.2 * \frac{180}{\pi}\right)-1}{1.2\,\tan\left(1.2 * \frac{180}{\pi}\right)}\right)\right]$$

$$\theta_B = 0.570114\,\frac{M_o L}{EI} \tag{17}$$

From equations (14) and (16):

$$\theta_{A\ (case\ 1)} = \theta_{A\ (case\ 2)}$$

From equations (15) and (17):

$$\theta_{B\ (case\ 1)} = \theta_{B\ (case\ 2)}$$

3. Buckling factor (K_{cr}) for composite girder with rigid far end in braced and unbraced frames

The value of the suggested buckling factor change generated by changing a number of parameters must be assessed, which requires the study of these parameters. These parameters are briefly described in the sentences that follow:

Table 3. Comparison between the rotation angles at the ends of the constant cross-section steel girder and the rotation angle equations of the composite girder at constant cross-sectional girder approach.

Equations from	Suggested formula	Reference (Stephen and Timoshenko, 1961)
θ_A	$\frac{M_o L}{EI}\left(\frac{1-\cos(2u)}{2u\sin(2u)}\right)$	$\frac{M_o L}{EI}\left(\frac{\Psi(u)}{3} + \frac{\phi(u)}{6}\right)$
θ_B	$\frac{M_o L}{EI}\left[\frac{\sin(2u)}{2u} + \left(\frac{\cos(2u)-1}{2u\tan(2u)}\right)\right]$	$\frac{M_o L}{EI}\left(\frac{\Psi(u)}{3} + \frac{\phi(u)}{6}\right)$

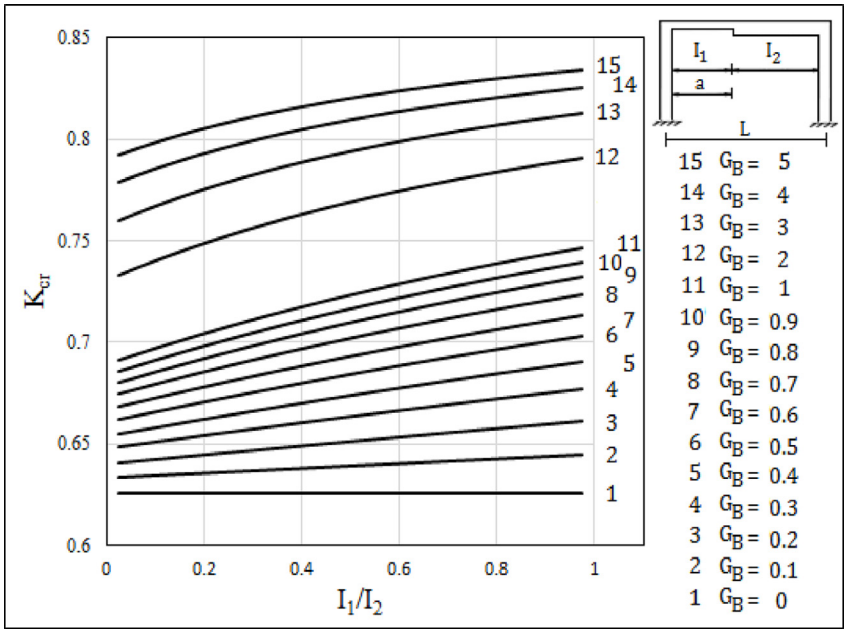

Fig. 3. Effective length factor for composite girder with hinged far end in braced frames (Fixed base) (a/L = 0.15).

(1) The adjustment of the column base, therefore we sometimes use a hinged base and sometimes a fixed base.
(2) The far end condition of the composite steel beam is hinged far end.
(3) Increasing the moment of inertia ratio (I_1/I_2) for the composite steel girder from 0.025 to 0.975 with two cases of braced and unbraced frames.

(a) After changing the column base from a fixed base to a hinged base, we observed that:
(1) According to the relationship between the moment of inertia ratio (I_1/I_2) and the suggested buckling factor (K_{cr}), the recommended buckling factor changed as follows:
    1) Figs. 3 and 4 represent a substantial growth in buckling factor of around 1.7%, rise as high as 7.1%.

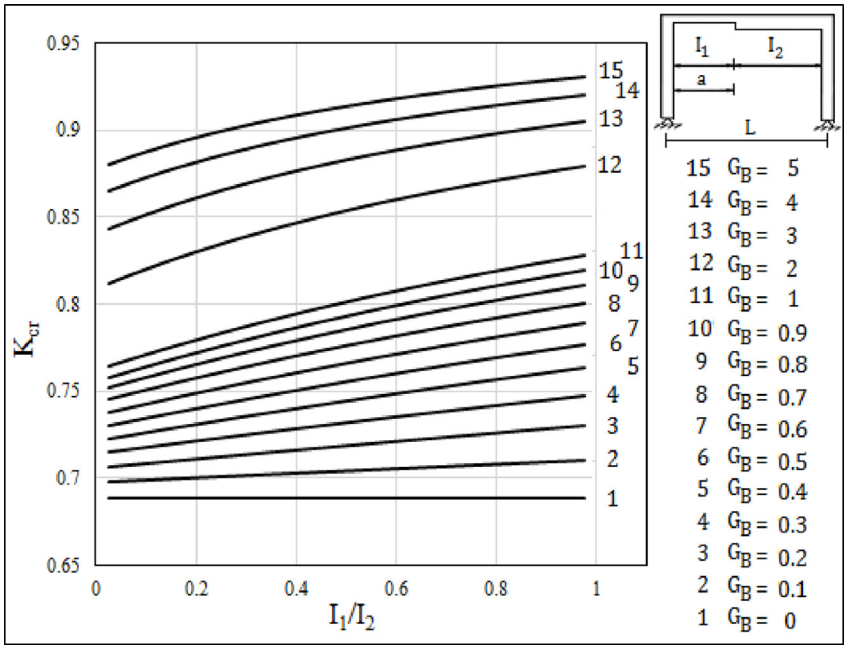

Fig. 4. Effective length factor for composite girder with hinged far end in braced frames (Hinged base) (a/L = 0.15).

2) Figs. 5 and 6 reveal a 22.86%–31.02% increase in buckling factor.

(2) There is a variance in the buckling factor as parameter (G_B) increases. The expression for this variant is:
   1) Figs. 3 and 4 indicate a significant increase of about 58.94%, reaching up to 117.15%.
   2) More about Figs. 5 and 6, it climbs from 5.45% by almost 19.07%.

Eventually, it becomes clear that the stiffness modification factor (α) is dependent on the length of the beam. However, when the moment of inertia ratio (I_1/I_2) becomes constant, we may ignore the beam length in the stiffness modification calculation.

4. Comparison between the buckling length factors "K" in the alignment chart equations and the proposed buckling length factors "$K_{proposed}$" for composite girder

Figures from (7) to (10) illustrate the values of the buckling length factors obtained from the alignment chart equations in the frame with the steel beam

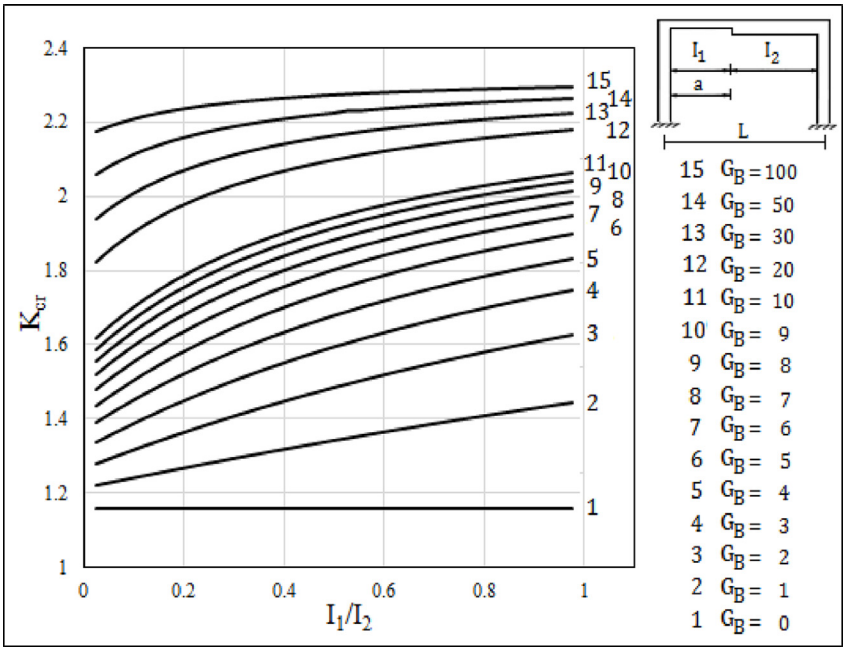

Fig. 5. Effective length factor for composite girder with hinged far end in unbraced frames (Fixed base) (a/L = 0.06).

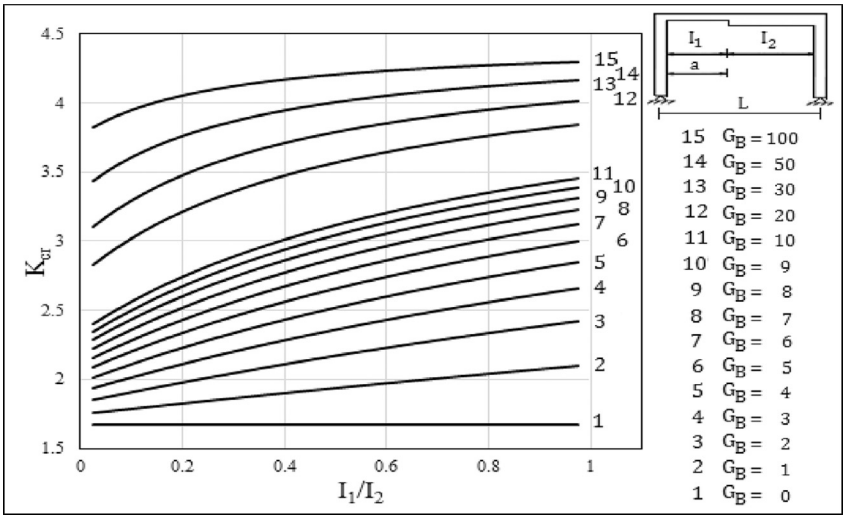

Fig. 6. Effective length factor for composite girder with hinged far end in unbraced frames (Hinged base) (a/L = 0.06).

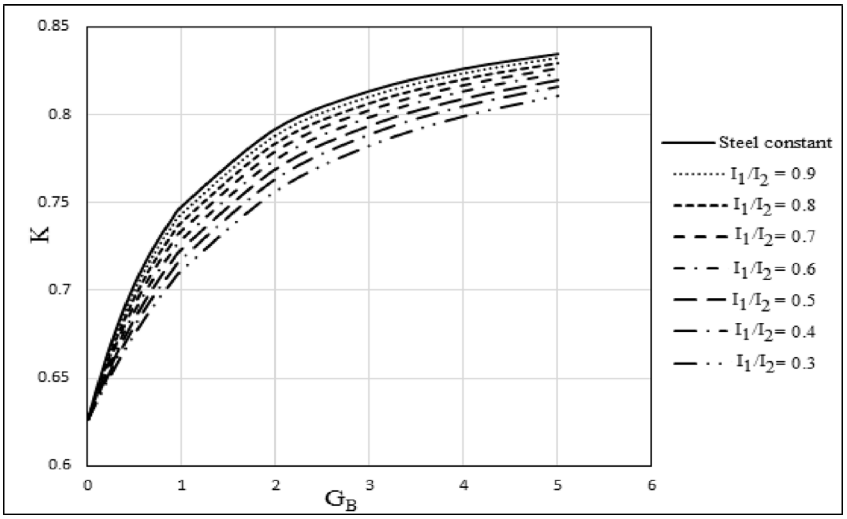

Fig. 7. Comparison between the values of the buckling length factors calculated from the alignment chart equations in the frame with the steel beam and the values estimated from the proposed buckling factor for composite girder with hinged far end condition in braced frames (Fixed base).

compared to the values estimated from the proposed formula in the frame with the composite beam. The tables demonstrate the difference between these values and their percentage.

1) In a prevented sway frame with a Hinged far end girder, the difference for buckling factor was between 0.172% and 7.228% when a fixed column base was employed as shown in Fig. 7.
2) If a hinged column base was used in a prevented sway frame with a hinged far end girder, the difference for buckling factor was around 0.181% and 7.519% as seen in Fig. 8.
3) The percentage of difference in buckling factor was anything from 0.123% to 26.811%

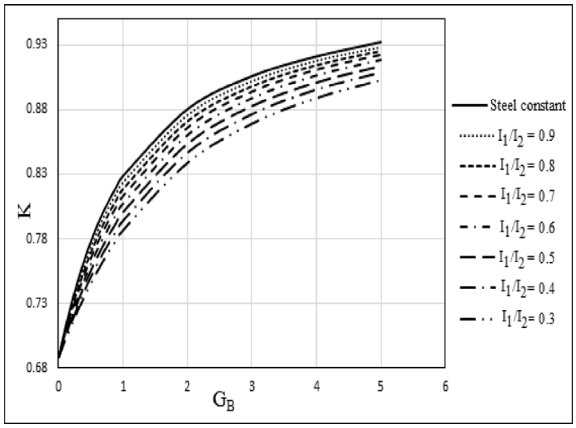

Fig. 8. Comparison between the values of the buckling length factors calculated from the alignment chart equations in the frame with the steel beam and the values estimated from the proposed buckling factor for composite girder with hinged far end condition in braced frames (Hinged base).

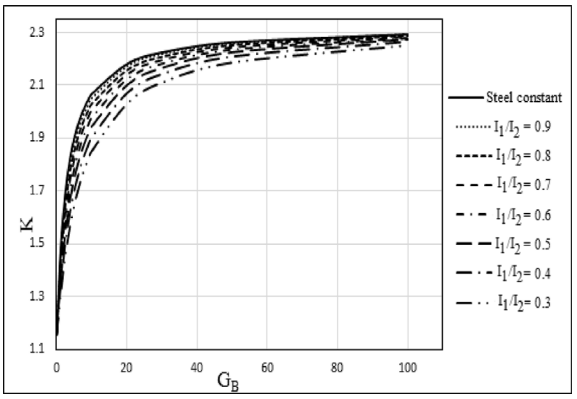

Fig. 9. Comparison between the values of the buckling length factors calculated from the alignment chart equations in the frame with the steel beam and the values estimated from the proposed buckling factor for composite girder with hinged far end condition in unbraced frames (Fixed base).

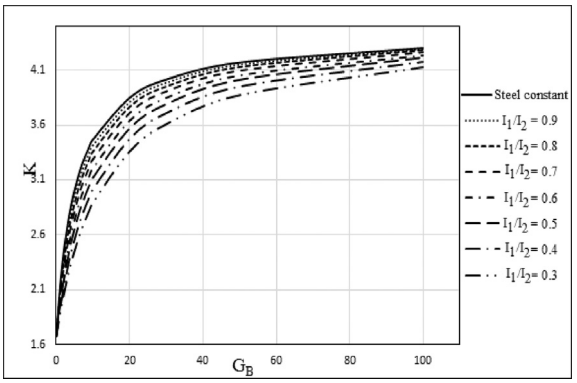

Fig. 10. Comparison between the values of the buckling length factors calculated from the alignment chart equations in the frame with the steel beam and the values estimated from the proposed buckling factor for composite girder with hinged far end condition in unbraced frames (Hinged base).

when it came to permitting sway columns in a frame with a hinged far end girder and where the column base was fixed as illustrated in Fig. 9.

4) If a hinged column base was included in a permitted sway frame with a hinged far end girder, the difference for buckling factor was around 0.294% and 37.214% as regarded in Fig. 10.

5. The relationship between the critical buckling factor and the beam length

From a broad perspective, a number of factors should be investigated to see how the proposed buckling factor varies when these values are changed. Here are some specifics about these parameters:

1) The composite steel beam's far end is designed with a hinged far end.
2) Changes to the column base. Both fixed and hinged bases are used.
3) The length of a composite girder is changed between 4 m and 15 m.
4) The side sway mode could be switched between prevented and permitted.

These figures show that when the proposed buckling factor increases, the beam length increase as well. Additionally, there is a growing trend in the buckling factor as the number of IPE sections rises.

(1) The outcome of employing a hinged base column as opposed to a fixed one is:

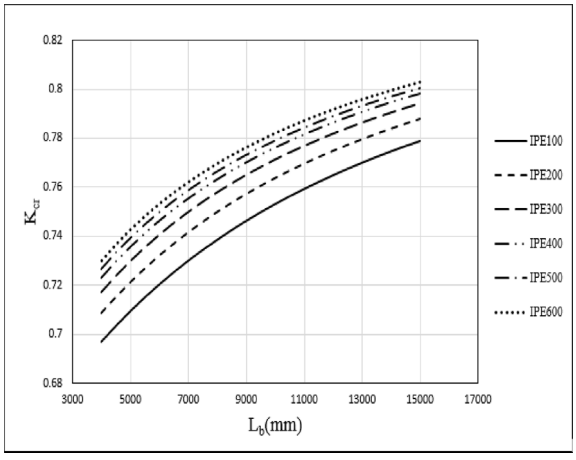

Fig. 11. The relationship between the critical buckling factor and the beam length in braced frame with fixed far end girder (a/L = 0.15, hinged base, center spacing = 2000 mm, t_c = 120 mm, E_c = 220 t/cm^2, $I_{col} = I_{steel\ beam}$).

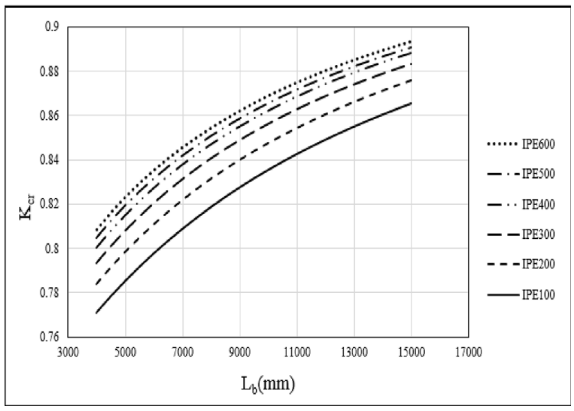

Fig. 12. The relationship between the critical buckling factor and the beam length in braced frame with hinged far end girder (a/L = 0.15, hinged base, center spacing = 2000 mm, t_c = 120 mm, E_c = 220 t/cm^2, $I_{col} = I_{steel\ beam}$).

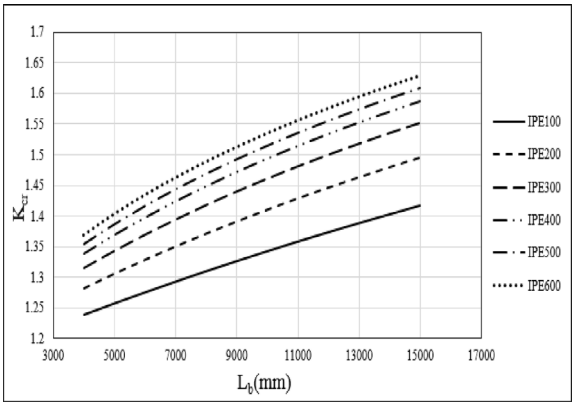

Fig. 13. The relationship between the critical buckling factor and the beam length in unbraced frame with hinged far end girder (a/L = 0.06, fixed base, center spacing = 2000 mm, t_c = 120 mm, E_c = 220 t/cm^2, $I_{col} = I_{steel\ beam}$).

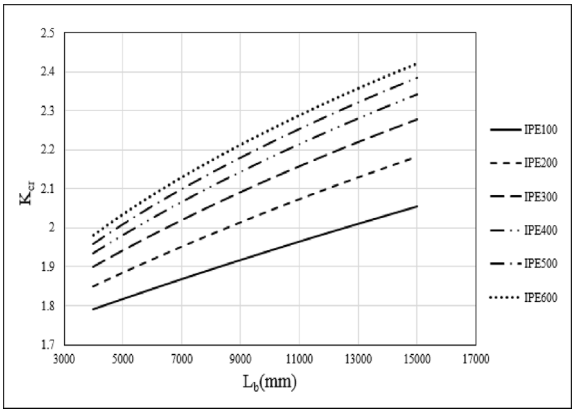

Fig. 14. The relationship between the critical buckling factor and the beam length in unbraced frame with hinged far end girder (a/L = 0.06, hinged base, center spacing = 2000 mm, t_c = 120 mm, E_c = 220 t/cm^2, $I_{col} = I_{steel\ beam}$).

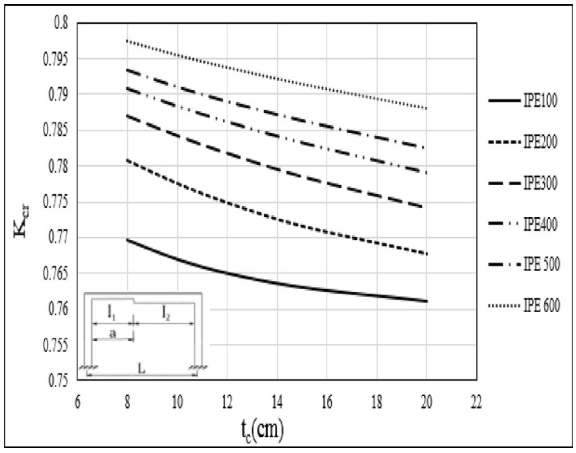

Fig. 15. The relationship between the critical buckling factor and the concrete slab thickness in braced frame with hinged far end girder a/L = 0.15 L, fixed base, L_{beam} = 12,000 mm, E_c = 220 t/cm^2, $I_{col} = I_{steel\ beam}$).

a) The suggested buckling factor (K_{cr}) has been modified as follows in response to the increase in the length of composite beams:
   1) Besides the results in Figs. 11 and 12, the buckling factor ramps up by about 10.27%, to 12.34%.
   2) Figs. 13 and 14 demonstrate that it has gone up by about 13.7% and can go as high as 20%.

b) As the number of IPE sections increases from 100 to 600, the buckling factor changes. The following details explain this variation:
   1) Figs. 11 and 12 show a considerable increase in buckling factor of roughly 3.2%, going up to 5%.
   2) In Figs. 13 and 14, it rises from 10.89% to around 17.07%.

6. The relationship between the critical buckling factor and the concrete slab thickness in braced and unbraced frame

From a general point of view, there are several parameters that should be studied to observe how much the proposed buckling factor changes when these parameters are altered. These parameters are detailed as followed:

1) A hinged far end is employed to adjust the far end condition of the composite steel beam.
2) Column base alteration. We utilize fixed and hinged base.
3) The side sway mode was toggled between both prevented and permitted.
4) The thickness of a concrete slab is changed between 8 cm and 20 cm.

As is seen from these charts, the buckling factors go down as the concrete slab thickness goes up. On top of that, there is a growing trend among all buckling factor curves with a surging IPE section number.

(1) The result of using a hinged base column rather than a fixed one:
   (a) As a result of the rise in slab concrete thickness for composite beams, the proposed buckling factor (Kcr) has adjusted as below:
      1) Including the results in Figs. 15 and 16, there is a ramp up in the buckling factor of nearly1.15%, up to 1.28%.
      2) Concerning Figs. 17 and 18, it goes up from 5.47% to about 5.01%.

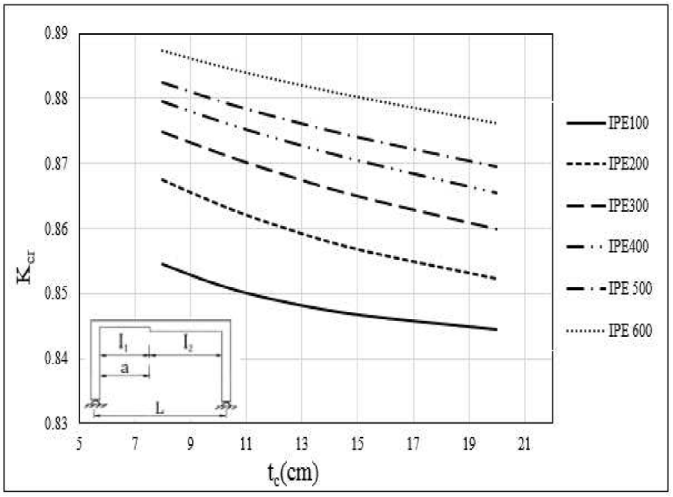

Fig. 16. The relationship between the critical buckling factor and the concrete slab thickness in braced frame with hinged far end girder a/L = 0.15 L, hinged base, L_{beam} = 12,000 mm, E_c = 220 t/cm^2, $I_{col} = I_{steel\ beam}$).

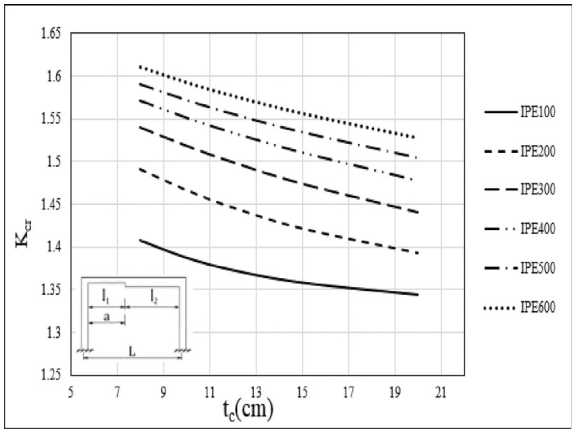

Fig. 17. The relationship between the critical buckling factor and the concrete slab thickness in unbraced frame with hinged far end girder (a/L = 0.06 L, fixed base, center spacing = 2000 mm, L_{beam} = 12,000 mm, E_c = 220 t/cm^2, $I_{col} = I_{steel\ beam}$).

(b) The buckling factor varies when the number of IPE sections climbs from 100 to 600. This difference is explained as follows:
1) Regarding Figs. 15 and 16, it grows from 3.6% to approximately 3.82%.
2) Figs. 17 and 18 reveal a 13.57–16.88% increase in buckling factor.

7. The relationship between the critical buckling factor and the modulus of elasticity in braced and unbraced frame

From an overall perspective, numerous parameters must be studied in order to determine the value of the proposed buckling factor change caused by modifying these parameters. The following points are a brief description of these parameters:

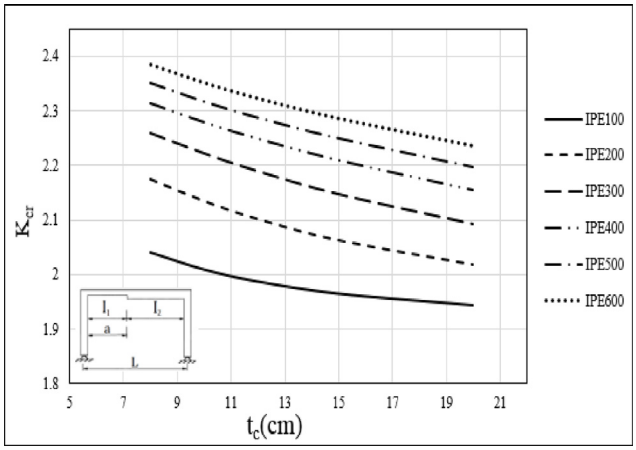

Fig. 18. The relationship between the critical buckling factor and the concrete slab thickness in unbraced frame with hinged far end girder (a/L = 0.06 L, hinged base, center spacing = 2000 mm, L_{beam} = 12,000 mm, E_c = 220 t/cm^2, $I_{col} = I_{steel\ beam}$).

1) The altering of the column base therefore we adopt a fixed base and occasionally a hinged base.
2) Toggling the modulus of elasticity of a concrete slab from 220 t/cm^2 to 310 t/cm^2.

As can be observed from the charts, there is a diminishing trend in buckling factor curves resulting from employing the IPE section number from IPE400 to IPE600 with a steadily increasing modulus of elasticity of slab concrete. Furthermore, there was also some fluctuation in buckling factor curves due to the use of the IPE section number ranging from IPE100 to IPE300 when the modulus of elasticity of slab concrete grows continuously. In addition, it is noticeable that more IPE section numbers in a composite girder means a higher proposed buckling factor.

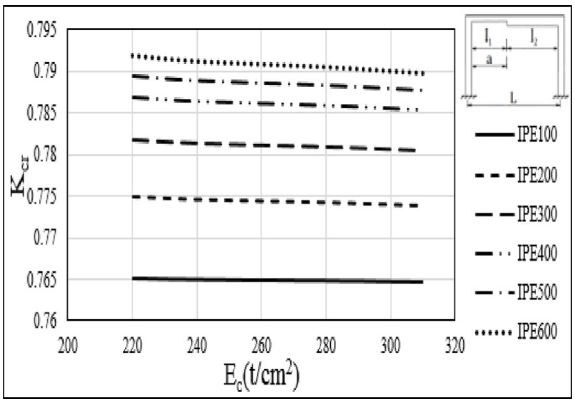

Fig. 19. The relationship between the critical buckling factor and the modulus of elasticity in braced frame with hinged far end girder, a/L = 0.15 L, fixed base, Lbeam = 12,000 mm, tc = 120 mm, Icol = Isteel beam.

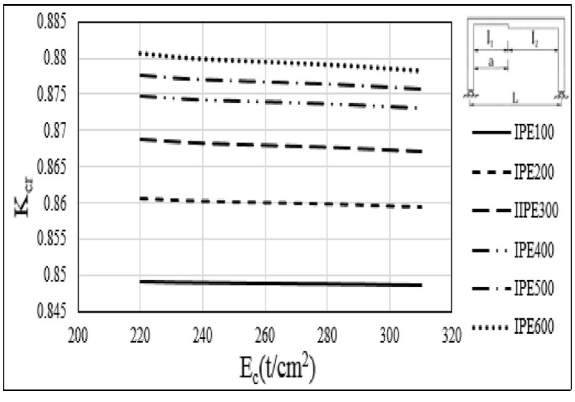

Fig. 20. The relationship between the critical buckling factor and the modulus of elasticity in braced frame with hinged far end girder, a/L = 0.15 L, hinged base, L_{beam} = 12,000 mm, t_c = 120 mm, $I_{col} = I_{steel\ beam}$.

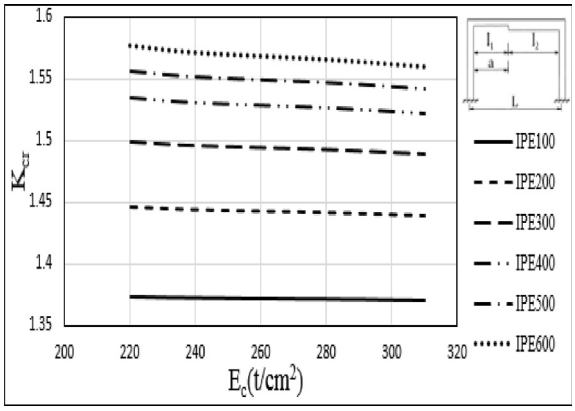

Fig. 21. The relationship between the critical buckling factor and the modulus of elasticity in unbraced frame with hinged far end girder, a/L = 0.06 L, fixed base, L_{beam} = 12,000 mm, t_c = 120 mm, $I_{col} = I_{steel\ beam}$.

(1) By converting the column base from a fixed base to a hinged base, we have come to the realization that:
   (a) According to the relation between the modulus of elasticity of a concrete slab and the proposed buckling factor (K_{cr}), the proposed buckling factor Changed as following:
      1) Figs. 19 and 20 demonstrate a significant rise in the buckling factor from around 0.05%–0.27%.
      2) Besides the results in Figs. 21 and 22, the buckling factor ramps up by about 0.2%, to 1.29%.
   (b) There is a variation in the buckling factor that occurs whenever the IPE section numbers are raised from IPE100 to IPE600. This variation is expressed as follows:
      1) Along with the data in Figs. 19 and 20, there is an almost 3.29% rise in the buckling factor, up to 4.72%.
      2) Figs. 21 and 22 show a considerable increase in buckling factor of roughly 13.81%, going up to 16.92%.

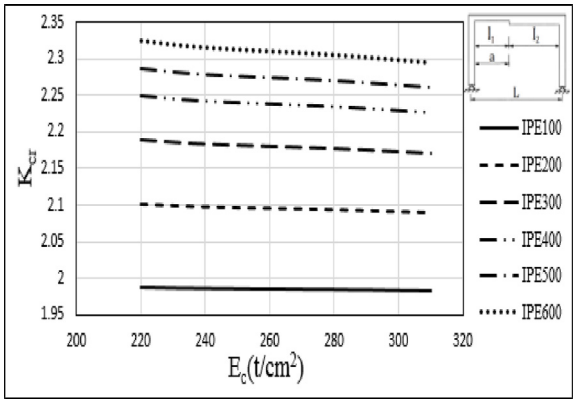

Fig. 22. The relationship between the critical buckling factor and the modulus of elasticity in unbraced frame with hinged far end girder, a/L = 0.06 L, hinged base, L_{beam} = 12,000 mm, t_c = 120 mm, $I_{col} = I_{steel\ beam}$.

8. Comparison between the buckling factor calculated from the proposed formula and the buckling factor estimated from the alignment chart for composite beams and steel beams, respectively, in braced and unbraced frames

Overall, the two-bay frame that has three columns, two composite beams with the same cross section was studied in the next charts. Initially, the buckling factor has been calculated for the middle column (A-B) in these charts. Moreover, the line graphs make it clear that the buckling factor curves steadily got higher as the beam length went from 4 m to 15 m. Additionally, the solid lines are the alignment chart solutions that resulted from using steel beams. Also, the dashed lines are the solutions from the proposed formula, and the dot-dashed lines are the solutions from the alignment chart when composite beams are used.

- As observed from Fig. 23, the ratio between the solid and dot-dashed lines is 1.04. However, the dashed line outclasses the dot-dashed lines by around 1.08.
- Concerning Fig. 24, the solid line outmatches the dot-dashed line by 1.05. Actually, the dashed line is above the dot-dashed line by approximately 1.09.

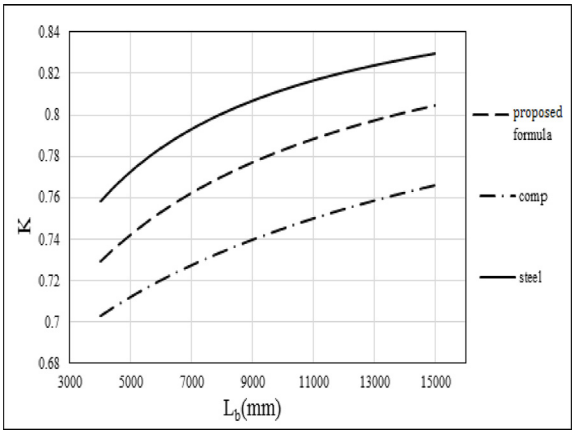

Fig. 23. Comparison between the buckling factor for braced frame with hinged far end girder, fixed base, t_c = 120 mm, E_c = 220 t/cm^2, L_{col} = 4000 mm, I_{col} = HEA340, $I_{steel\ beam}$ = IPE330, center spacing = 3000 mm, two bays frame.

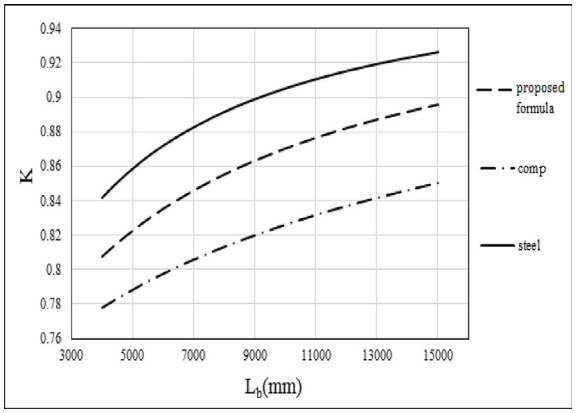

Fig. 24. Comparison between the buckling factor for braced frame with hinged far end girder, fixed base, t_c = 120 mm, E_c = 220 t/cm^2, L_{col} = 4000 mm, I_{col} = HEA340, $I_{steel\ beam}$ = IPE330, center spacing = 3000 mm, two bays frame.

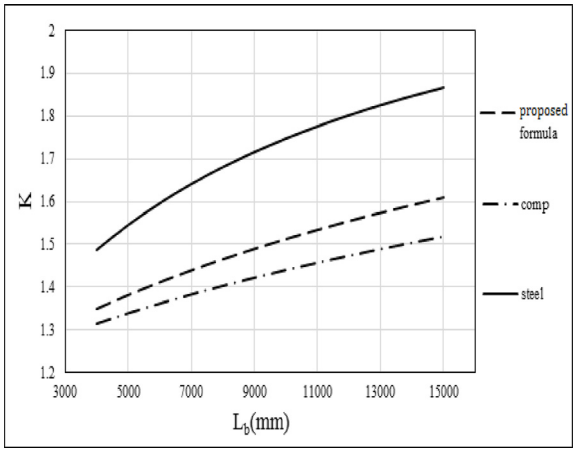

Fig. 25. Comparison between the buckling factor for unbraced frame with hinged far end girder, fixed base, t_c = 120 mm, E_c = 220 t/cm^2, L_{col} = 4000 mm, I_{col} = HEA340, $I_{steel\ beam}$ = IPE330, center spacing = 3000 mm, two bays frame.

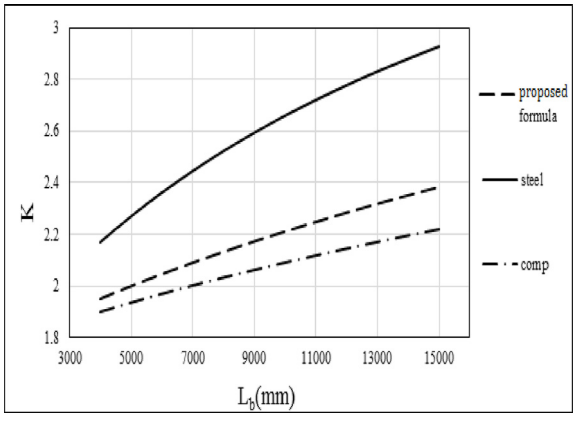

Fig. 26. Comparison between the buckling factor for unbraced frame with hinged far end girder, hinged base, t_c = 120 mm, E_c = 220 t/cm^2, L_{col} = 4000 mm, I_{col} = HEA340, $I_{steel\ beam}$ = IPE330, center spacing = 3000 mm, two bays frame.

- from Fig. 25, we can clearly notice that the ratio between the solid and dot-dashed lines is 1.04. Furthermore, the dashed line outpaces dot-dashed line by about 1.18.
- In Fig. 26 as well, the solid is above dot-dashed lines by 1.05. Eventually, the ratio of the dashed to dot-dashed lines is 1.23.

9. Conclusions and summary

This paper demonstrates the effective length factor calculation method for columns in braced and unbraced frames with composite girders. The condition of the girder's far end is represented as hinged. In addition, the equations for the proposed buckling factor have been proven using parameter-based methods (α). Moreover, the closed form of the parameter (α) has been determined. Furthermore, we compare the values of the buckling length factors calculated from the alignment chart equations in the frame with the steel beam with hinged far end condition and the values estimated from the proposed formula for composite girder with hinged far end condition in both braced and unbraced frames. Additionally, the relationship between the proposed buckling factor and beam length has been clarified. Also, we study the influence of changing the slab thickness from 8 cm to 20 cm on the suggested buckling factor. In both braced and unbraced frames, the relationship between the critical buckling factor and the modulus of elasticity has been examined. On top of that, we show the comparison between the buckling factor calculated from the proposed formula and the buckling factor estimated from the alignment chart for composite beams and steel beams, respectively, in braced and unbraced frames.

Finally, a number of inferences may be drawn from the results of the current study as well as these results are summarized below:

1. When we compare the values of the buckling length factors obtained from the alignment chart equations in the frame with the steel beam and the values estimated from the proposed formula in the braced frame with the composite, we find that the percentage of difference for side sway prevented frame ranged from 0.172% to 7.519%.
2. Furthermore, the difference between the values of the buckling length factors calculated from the alignment chart equations in the frame with the steel beam and the values estimated from the proposed formula in the unbraced frame with the composite beam ranged from −0.123% to 37.214% for the side sway permitted columns in the frame.

3. Concerning braced and unbraced frame, it's clear that the ratio between the moment of inertia ratio (I_1/ I_2) and the proposed buckling factor (K_{cr}) grows progressively by using a hinged column base instead of a fixed one when all other studied parameters remain constant.
4. While all other examined parameters stay constant, the proposed buckling factor (K_{cr}) moderately rises when the parameter (G_B) grows as a consequence of altering the composite beam's far end from rigid to fixed.
5. Regarding the unbraced frame, it's remarkable that the relationship between the length of the composite beam and the proposed buckling factor (K_{cr}) increases gradually when changing the column base from hinged to fixed.
6. Furthermore, whenever the IPE section number grows, the proposed buckling factor rises as well.
7. Obviously, the result of using an unbraced frame instead of a braced one demonstrate that there is a significantly growing in the proposed K-parameter (K_{cr}) with the gradual lengthening of the composite beam.
8. Consequently, there is a diminishing trend in proposed buckling factor curves resulting from employing the IPE section number from IPE400 to IPE600 with a steadily increasing modulus of elasticity of slab concrete. Furthermore, there was also some fluctuation in buckling factor curves due to the use of the IPE section number ranging from IPE100 to IPE300 when the modulus of elasticity of slab concrete grows continuously.
9. It must be noted that, the proposed buckling factor curves go down as the slab thickness goes up.
10. Graphed charts make it easier to follow design procedures.

Authors contribution

The research strategies were devised by N.S. Mahmoud and S.M. Abdrabou. S.A.Eltawil compiled the research data, modified the buckling factor formula for columns in braced and unbraced frames with composite girders, and drew charts. N.S. Mahmoud and S.M. Abdrabou supervised the derivation and conducted out the observations. At all stages, the authors discussed and checked the chart's results, as well as commented on that results. The solved example consequences were analyzed by N.S. Mahmoud, S.M. Abdrabou, and S.A. Eltawil. The paper was written and edited by S.A. Eltawil under the supervision of N.S. Mahmoud and S.M. Abdrabou. The work reported in this publication was equally contributed by all authors. The paper's published version has been reviewed and approved by all authors.

Funding statement

Funding for this research was a personal funding.

Conflicts of interest

The author has no conflict of interest.

Appendix

Parameters V, Y, Z, and Q are given by:

$$V=\left(\frac{\cos(K_1a)-1}{K_1^2L^2\cos(K_1a)}+\frac{\tan(K_1a)}{K_1L}+\frac{1}{rK_2^2L^2\cos(K_1a)}+\left(g*\frac{K_2\sin(K_2a)\tan(K_2L)+K_2\cos(K_2a)}{\cos(K_1a)}*\left(\frac{K_1a-K_1L-\tan(K_1a)}{rK_2^2K_1L^2}+\frac{1-\cos(K_1a)-\tan(K_1a)\sin(K_1a)}{K_1^2L}+\frac{\tan(K_1a)-K_1a}{K_1^3L^2}\right)\right)\right)$$

$$Y=\left(\frac{1-\cos(K_1a)}{K_1^2L^2\cos(K_1a)}-\frac{\sin(K_2a)}{rK_2L\cos(K_2L)\cos(K_1a)}-\frac{1}{rK_2^2L^2\cos(K_1a)}+\left(g*\frac{K_2\sin(K_2a)\tan(K_2L)+K_2\cos(K_2a)}{\cos(K_1a)}*\left(\frac{\cos(K_2a)}{rK_2^2L\cos(K_2L)}-\frac{a}{rK_2^2L^2}-\frac{\tan(K_1a)}{K_1^3L^2}+\frac{\tan(K_1a)\sin(K_2a)}{rK_2K_1L\cos(K_2L)}+\frac{\tan(K_1a)}{rK_2^2K_1L^2}+\frac{a}{K_1^2L^2}\right)\right)\right)$$

$$Z=\left(\left(gK_2\sin(K_2L)\tan(K_2L)*\left(\frac{a}{rK_2^2L^2}-\frac{1}{rK_2^2L}-\frac{\cos(K_1a)}{K_1^2L}+\frac{\tan(K_1a)}{K_1^3L^2}-\frac{\tan(K_1a)\sin(K_1a)}{K_1^2L}-\frac{\tan(K_1a)}{rK_2^2K_1L^2}-\frac{a}{K_1^2L}+\frac{1}{K_1^2L}\right)\right)+\left(gK_2\cos(K_2L)*\left(\frac{a}{rK_2^2L^2}-\frac{1}{rK_2^2L}-\frac{\cos(K_1a)}{K_1^2L}+\frac{\tan(K_1a)}{K_1^3L^2}-\frac{\tan(K_1a)\sin(K_1a)}{K_1^2L}-\frac{\tan(K_1a)}{rK_2^2K_1L^2}-\frac{a}{K_1^2L}+L\frac{1}{K_1^2}\right)\right)+\frac{1}{rK_2^2L^2}\right)$$

$$Q = \left(\left(gK_2 \sin(K_2L) \tan(K_2L) * \left(\frac{\cos(K_2a)}{rK_2{}^2L\cos(K_2L)} - \frac{a}{rK_2{}^2L^2} - \frac{\tan(K_1a)}{K_1{}^3L^2} + \frac{\tan(K_1a)\sin(K_2a)}{rK_2K_1L\cos(K_2L)} + \frac{\tan(K_1a)}{rK_2{}^2K_1L^2} + \frac{a}{K_1{}^2L^2} \right) \right) + \left(g\,K_2\cos(K_2L) * \left(\frac{\cos(K_2a)}{rK_2{}^2L\cos(K_2L)} - \frac{a}{rK_2{}^2L^2} - \frac{\tan(K_1a)}{K_1{}^3L^2} - \frac{\tan(K_1a)\sin(K_2a)}{rK_2K_1L\cos(K_2L)} + \frac{\tan(K_1a)}{rK_2{}^2K_1L^2} + \frac{a}{K_1{}^2L^2} \right) \right) + \frac{\tan(K_2L)}{rK_2L} + \frac{1}{rK_2{}^2L^2} \right)$$

$$g = \frac{1}{t}$$

$$t = \left(\frac{\tan(K_1a)}{K_1} (K_2 \sin(K_2a) \tan(K_2L) + K_2\cos) \times (K_2a) + \cos(K_2a)\tan(K_2L) - \sin(K_2a) \right)$$

Where:

$$K = \sqrt{\frac{P}{EI}}$$

$$r = \frac{I_2}{I_1}$$

References

AISC, 2010. Specification for Structural Steel Buildings, ANSI/AISC 360-16. Am. Inst. Steel Constr., p 676

Al-Ghalibi, F.Y., 2014. Effective length factor for column in frame with girders on elastic foundation. J. Sci. Eng. Res. 5 (December 2014), 1259–1270.

Ali, E.H.A.H., 2012. Establishing a New Simple Formula for Buckling Length Factor (K) of Rigid Frames Columns, vol. 6, pp. 42–52. https://doi.org/10.5281/zenodo.1073517, 1.

Bradford, M.A., Manh, H.V., Gilbert, R.I., 2002. Numerical analysis of continuous composite beams under service loading. Adv. Struct. Eng. 5 (1), 1–12. https://doi.org/10.1260/1369433021502498.

Chang, G., Meng, Y., Niu, B., 2017. Research of Cracking Moment in Negative Moment Area of the Steel-Concrete Continuous Beam, vol. 76. Emim, pp. 1372–1376. https://doi.org/10.2991/emim-17.2017.274.

Chen, J., Jiang, A., Jin, W., 2014. Behavior of steel-concrete composite beams with corroded shear studs under negative bending moment. Proc. 4th Int. Conf. Durab. Concr. Struct. ICDCS 2014 (July), 127–136. https://doi.org/10.5703/1288284315393.

da Silva, L.S., Simões, R., Gervásio, H., 2010. Eurocode 3: Part 1-1. General rules and rules for buildings 3 (1). https://doi.org/10.1002/9783433601099. Available.

Duan, L., Chen, W.F., 1999. Effective Length of Compression Members. CRC Press LLC, 2003.

Fan, J., Nie, X., Li, Q., Li, Q., 2010. Long-term behavior of composite beams under positive and negative bending. II: analytical study. J. Struct. Eng. 136 (7), 858–865. https://doi.org/10.1061/(asce)st.1943-541x.0000176.

Girgin, K., Özmen, G., 2008. Effective lengths of braced frame columns. Struct. Eng. Mech. 28 (2), 189–206. https://doi.org/10.12989/sem.2008.28.2.189.

Johnson, R., 2011. Designers Guide to Eurocode 4: Design of Composite Steel and Concrete Structures, second ed. Second. ICE Publishing, 40 Marsh Wall, London E14 9TP Full.

King, W.S., Duan, L., Zhou, R.G., Hu, Y.X., Chen, W.F., 1993. K-factors of framed columns restrained by tapered girders in US codes. Eng. Struct. 15 (5), 369–378. https://doi.org/10.1016/0141-0296(93)90040-B.

Korkess, I.N., Yousifany, A.H., Abdul-majeed, Q., Husain, H.M., 2009. Behavior of composite steel-concrete beam subjected to negative bending. Eng. Techonol. 27 (1), 53–72.

Kostic, S., Deretic-Stojanovic, B., Stosic, S., 2011. Redistribution effects in linear elastic analyses of continuous composite steel-concrete beams according to Eurocode 4. Facta Univ. – Ser. Archit. Civ. Eng. 9 (1), 133–145. https://doi.org/10.2298/fuace1101133k.

Lian Duan, A., Chen, Wai-Fah, 1989a. EFFECTIVE LENGTH FACTOR FOR COLUMNS IN BRACED FRAMES, 2 Member, vol. 114, p. 2357 2370. https://doi.org/10.1061/(ASCE)0733-9445(1988)114:10(2357). no. 10.

Lian Duan, A., Chen, Wai-Fah, 1989b. 2 Member, "effec -tive length factor for columns in unbraced frames by Lian Duan 1 and Wai-Fah Chen, 2 Member. ASCE 115 (1), 149–165. https://doi.org/10.1061/(ASCE)0733-9445(1989)115:1(149).

M. of Housing, 2001. Egyptian Code of Practice for Steel Construction and Bridges. Allowable Stress Design, 205.

M. of Housing, 2007. Egyptian Code of Practice for Steel Construction (Load and Resistance Factor Design) (LRFD). no. 359.

Mbc, W., 2014. Composite Slabs and Beams Using Steel Decking : Best Practice for Design and Construction. Revised Edition, 13.

Moustafa, A., Salama, M.I., 2015. Effective length factor fo. IOSR J. Mech. Civ. Eng. Ver. II 12 (3), 66–71. https://doi.org/10.9790/1684-12326671.

Nie, J., Fan, J., Cai, C.S., 2004. Stiffness and deflection of steel–concrete composite beams under negative bending. J. Struct. Eng. 130 (11), 1842–1851. https://doi.org/10.1061/(asce)07339445(2004)130:11(1842).

Stephen, J.M.G., Timoshenko, P., 1961. Theory of Elastic Stability by S. Timoshenko and Jmgere 1963.Pdf, second. mcgraw-hill international book company.

Tikka, T.K., Mirza, S.A., 2014. Effective length of reinforced concrete columns in braced frames. Int. J. Concr. Struct. Mater. 8 (2), 99–116. https://doi.org/10.1007/s40069-014-0070-7.

Vasdravellis, G., Uy, B., Tan, E.L., Kirkland, B., 2012. Behaviour and design of composite beams subjected to negative bending and compression. J. Constr. Steel Res. 79, 34–47. https://doi.org/10.1016/j.jcsr.2012.07.012.

Webber, A., Orr, J.J., Shepherd, P., Crothers, K., 2015a. The effective length of columns in multi-storey frames. Eng. Struct. 102 (2015), 132–143. https://doi.org/10.1016/j.engstruct.2015.07.039.

Webber, A., Orr, J.J., Shepherd, P., Crothers, K., 2015b. The effective length of columns in unbraced frames. Eng. Struct. 102, 132–143. https://doi.org/10.1016/j.engstruct.2015.07.039.

عنوان البحث باللغة العربية
الجزء الثانى: معامل الإنبعاج المقترح للأعمدة في الإطارات المقيدة والغير مقيدة ذات الكمرات المركبة.

الملخص باللغة العربية
في البحث الحالى ، تم دراسة تأثير الكمرات المركبة على القيم المقترحة لمعامل الإنبعاج الخاص بالأعمدة في الإطارات المقيدة والغير مقيدة حيث تم تمثيل الركائز البعيدة للكمرات المركبة على أنها مفصلية. علاوة على ذلك ، تعتمد الصيغ المشتقة على معاملات الصلابة المعدلة وتتبع نفس الإفتراضات المتبعة في حساب معامل الطول الفعال القياسي. بالإضافة إلى ذلك ، تم استخدام طريقة الانحراف الانحدارى للحصول على صيغ مقترحة لمعامل الإنبعاج الخاص بالأعمدة في الإطارات ذات الكمرات المركبة سواء كانت إطارات مقيدة أوغير مقيدة. فيما يتعلق بالإطار غير المقيد ، فإن معامل الانحناء المقترح للأعمدة الغير مقيدة بواسطة الكمرات المركبة يدقق من الطول الفعال ويجعله تصميم أكثر دقة وفعالية من حيث التكلفة من معامل التواء الأعمدة المقيّد بواسطة الكمرات الفولاذية. وأخيرًا ، هناك تحسن طفيف في معامل الانحناء المقترح للأعمدة في الإطارات المقيدة باستخدام الكمرات المركبة مقارنة بمعامل التواء الأعمدة المقيدة بواسطة الكمرات الفولاذية ، ولكن لا يزال هناك دقة أعلى من الحل التقليدي.